Mechanism of termination of DNA replication of *Escherichia coli* involves helicase–contrahelicase interaction

Sashidhar Mulugu*, Aardra Potnis*, Shamsuzzaman*, Jeffery Taylor†, Ken Alexander‡, and Deepak Bastia*§

Departments of *Microbiology, †Biochemistry, and ‡Pediatrics, Duke University Medical Center, Durham, NC 27710

Edited by Nicholas R. Cozzarelli, University of California, Berkeley, CA, and approved June 22, 2001 (received for review February 7, 2001)

Using yeast forward and reverse two-hybrid analyses, we have discovered that the replication terminator protein Tus of *Escherichia coli* physically interacts with DnaB helicase *in vivo*. We have confirmed this protein–protein interaction *in vitro*. We show further that replication termination involves protein–protein interaction between Tus and DnaB at a critical region of Tus protein, called the L1 loop. Several mutations located in the L1 loop region not only reduced the protein–protein interaction but also eliminated or reduced the ability of the mutant forms of Tus to arrest DnaB at a *Ter* site. At least one mutation, E49K, significantly reduced Tus–DnaB interaction and almost completely eliminated the contrahelicase activity of Tus protein *in vitro* without significantly reducing the affinity of the mutant form of Tus for *Ter* DNA, in comparison with the wild-type protein. The results, considered along with the crystal structure of Tus–*Ter* complex, not only elucidate further the mechanism of helicase arrest but also explain the molecular basis of polarity of replication fork arrest at *Ter* sites.

protein–protein interaction | replication arrest | two-hybrid analysis | reverse two-hybrid analysis

Replication termination of prokaryotic and of some eukaryotic chromosomes occurs at specific sequences called replication termini (1, 2). In *Escherichia coli*, there are 10 replication termini (*Ter*) located in a region diametrically opposite to the replication origin (Fig. 1). The *Ter* sites have polarity, i.e., they arrest replication forks, when they are present in one orientation with respect to *ori*, but allow forks to pass through unimpeded in the opposite orientation (3–8). The *Ter* sites are located in two clusters of 5 each, with each cluster having a polarity opposite to that of the other. Thus, the arrangement of the *Ter* sites forms a replication trap that forces the two forks, initiated at *oriC*, to meet each other within a well-defined region of the chromosome (Fig. 1).

The *Ter* sites specifically interact with the replication terminator protein called Tus, which is a polar contrahelicase, i.e., it impedes the DNA unwinding activity of DnaB in an orientation-dependent manner (5, 6). The crystal structure of the Tus–*Ter* complex has been solved, and it reveals a bilobed protein that has structural asymmetry and has a DNA-binding domain, consisting of a series of β-strands, that invade the major groove of *Ter* DNA (Fig. 2 and ref. 8). The crystal structure was originally interpreted to account for replication fork arrest, solely on the basis of Tus–*Ter*, protein–DNA interaction, that supposedly was strong enough to form a nonspecific barrier, not only to DnaB helicase-catalyzed DNA unwinding, but also, in principle, to any protein that would unwind DNA (8). Existing biochemical data were also interpreted to suggest such a simplistic ''roadblock'' model for replication fork arrest at the *Ter* sites (6).

The roadblock model seems to be unsatisfactory for several reasons. First, the bacterial chromosome does not exist *in vivo* as naked DNA but is coated with various DNA-binding proteins, some of which bind to DNA with strong affinity (9). Yet, replication forks apparently have the ability to pass through the various DNA–protein complexes present on the chromosome,

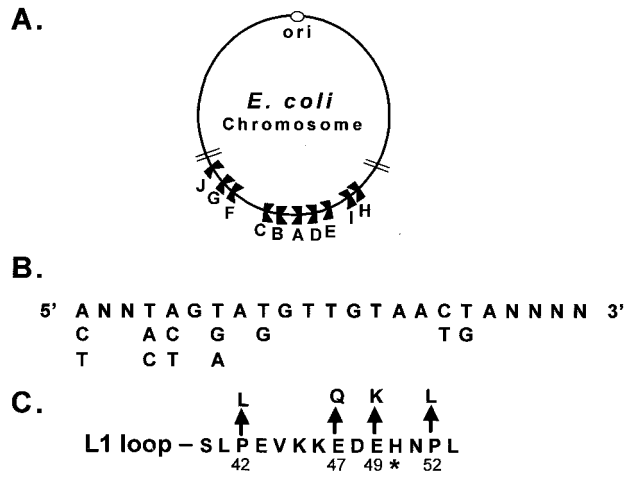

Fig. 1. Locations and sequences of the replication termini of *E. coli*. (*A*) Map showing the *ori* and the 10 *Ter* sites. (*B*) The consensus sequence of *Ter*. (*C*) Location of the mutations in the L1 loop of Tus that were investigated in the present work. The asterisk shows the location of the single protein-sugar-phosphate contact at H50.

and are arrested efficiently only at replication termini. Second, the Tus protein shows some helicase specificity in that it arrests replicative helicases such as DnaB, simian virus 40 T antigen, and RNA polymerases, but does not arrest helicase II or Rep helicases (5–7, 10, 11, 17, 18). Neither this specificity, albeit of a broad range, nor the polarity issue appeared to be consistent with the passive roadblock model.

Although mutagenesis of the Tus protein has been carried out previously, and mutants that were defective in replication termination *in vivo* were identified, the mechanism of replication termination had remained unclear because the previous work could neither definitively support nor rule out the possibility of Tus–DnaB interaction as a possible mechanistic element in replication fork arrest (9, 12, 13). In this paper, we use yeast forward two-hybrid analysis (14, 15) to show that Tus interacts *in vivo* with DnaB. The interaction between Tus and DnaB has also been confirmed *in vitro* by two different methods.

The specificity of the Tus–DnaB interaction was investigated by performing reverse yeast two-hybrid analysis that yielded a single missense mutation (P42L) located in the L1 loop of Tus. The mutant form of the protein was markedly deficient in interacting with DnaB *in vitro*. The result prompted us to isolate

This paper was submitted directly (Track II) to the PNAS office.

Abbreviations: wt, wild type; AT, 3-aminotriazol; Tag, T antigen; GST, glutathione *S*-transferase.

§To whom reprint requests should be addressed. E-mail: basti002@mc.duke.edu.

The publication costs of this article were defrayed in part by page charge payment. This article must therefore be hereby marked "*advertisement*" in accordance with 18 U.S.C. §1734 solely to indicate this fact.

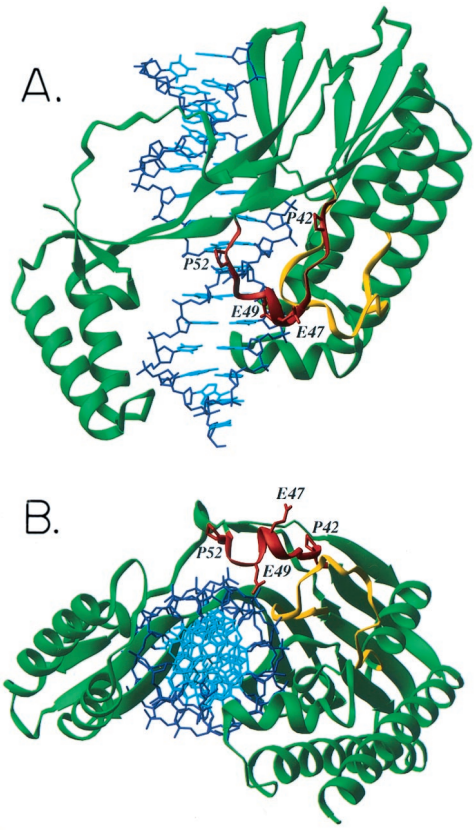

Fig. 2. The crystal structure of the *Ter* DNA–Tus protein complex (8) showing the nonblocking and the fork-blocking faces of Tus. (*A*) The L1 (red) and L2 (yellow) loops are shown along with the locations of four of the mutants. Note that the L1 loop is projecting from the helicase-blocking surface and is available for contact with the DnaB helicase. (*B*) A cross-sectional view of the helicase-arresting surface.

additional site-directed mutants in the L1 loop, namely E47Q, E49K, and P52L. All of these mutant forms of Tus were defective in Tus–DnaB interaction *in vitro*. The E47Q and E49K forms bound almost as strongly to *Ter* DNA as the wild-type (wt) protein, whereas P42L and P52L showed reduced binding. All excepting one (E47Q) of the mutant forms of Tus were also defective in arresting DNA unwinding *in vitro*, catalyzed by DnaB helicase. The E49K, but not the E47Q mutant form, was also defective in arresting replication forks *in vitro*. Thus, the data presented here strongly support a model of replication termination that involves both Tus–*Ter* DNA–protein interaction and Tus–DnaB protein–protein interaction. Our results also explain how polarity is generated with regard to the direction of replication fork arrest at *Ter* sites.

Materials and Methods

Bacterial Strains and Plasmids. The *E. coli* strains DH5α [F′ *supE44*, *lacU169* (80 *lacZ* ΔM15), *hsdR17*, *recA1*, *endA1*, *gyrA96*, *thi-1*, *relA1*] was used for cloning, and BL21{DE3}[F-*ompT*, *hsdS*, (rB$^-$, mB$^-$)] containing the plasmid pLysS was used for expressing proteins in pET vectors (Novagen). The yeast strain PJ69–4A [*MAT***a** *trp1*-901 *leu2-3,112 ura3-52 his3-200 gal4 gal80 LYS*2::*GAL1-HIS3 GAL2-ADE2 met*::*GAL7-lac*Z] was used for two-hybrid assays (15).

Plasmid Constructions. pGAD-DnaB was constructed as follows. DnaB was PCR-amplified and cloned as an *Eco*RI/*Pst*I fragment in the pGAD424 plasmid. For pGBT-Tus, Tus was cloned as an *Eco*RI fragment in pGBT9 plasmid. pGAD-DnaG was constructed by amplifying *dnaG* by PCR and cloning it as an *Eco*RI/*Pst*I fragment into the pGAD424 plasmid. For Tus mutants, random mutations in the Tus gene were introduced by using error-prone PCR, and these PCR fragments were cloned as *Eco*RI/*Pst*I fragments in the pGBT9 plasmid. For expression of the mutant Tus protein, the 0.9-kb P42L was amplified by using Tus sequence-specific primers and cloned as a *Eco*RI/blunt fragment into *Eco*RI/*Sma*I sites of pGEX4T1 plasmid.

The pUC18-R6Kter and pUC19-R6Kter plasmids that were used as templates in the *in vitro* replication reactions have been described (5).

Yeast Two-Hybrid Procedure and Extraction and Recovery of Plasmid DNA from Yeast. Yeast transformation and two-hybrid selection was carried out using the host strain PJ69–4A. Protocols used were as described in ref. 15 and in the *Yeast Protocols Handbook* (CLONTECH).

Random and Site-Directed Mutagenesis of Tus and Isolation of Noninteracting Mutant Form of Tus. Tus DNA fragment was amplified by error-prone PCR using Amplitaq (Perkin-Elmer) in the presence of 1 mM $MnCl_2$. The PCR product was amplified in the presence of $MgCl_2$, the DNA product was ligated to pGBT9 plasmid as *Eco*RI/*Pst*I fragments, and the ligation mix was digested with *Bam*HI to remove any self-ligated vector molecules. This mix was transformed into *E. coli* and plasmid DNA was extracted from a pool of the transformants. The DNA pool was then transformed into PJ69–4A yeast cells containing the pGAD-DnaB plasmid, and transformants were selected on Leu$^-$ Trp$^-$ plates. Several transformants were streaked on Leu$^-$ and Trp$^-$, and His$^-$, Leu$^-$, and Trp$^-$ plus 2 mM 3-aminotriazol (AT) plates. Colonies not growing on Leu$^-$, Trp$^-$, His$^-$ plus 2 mM AT plates were streaked on His, Leu, Trp, Ade$^-$ plates. Of the 300 colonies that were picked, only 5 showed no growth on plates containing 2 mM AT but lacking leucine, histidine, and tryptophan and a second type of plates lacking leucine, tryptophan, and adenine. DNA was extracted from each of these 5 clones (as described earlier). PCR amplification of DNA from yeast cells auxotrophic for histidine and adenine was done by using Tus-specific primers and amplified the 0.9-kb Tus fragment. The Tus fragments from various noninteracting yeast cells were sequenced by using the ThermoSequenase Radiolabeled Terminator Cycle Sequencing kit from United States Biochemical.

Site-directed mutagenesis was carried out by using complementary primer pairs, both having a base mismatch (with respect to wt DNA) at the same position. The primer pairs were hybridized to template DNA and extended by PCR using *Pfu* DNA polymerase. The residual wt template DNA was digested away with *Dpn*I and the product was transformed into *E. coli* according to the manufacturer's handbook (QuikChange mutagenesis kit, Stratagene).

Purification of DnaB, Tus Protein, and Helicase Assay. The procedures have been described (5).

DNA-Binding Curves. To determine the relative oligonucleotide-binding affinities for wt and mutant Tus proteins, Ter oligonucleotide gel-shift band intensities were quantified by using a PhosphorImager. Ter oligonucleotide band intensity data were then used to calculate the proportions of protein-shifted and unshifted oligonucleotide. From these data, the proportion of shifted oligonucleotide could be determined as a function of the free wt Tus/mutant-Tus protein concentration. These data were then fitted to a rectangular hyperbolic form of the Michaelis–Menten equation using a nonlinear Newton-G iterative least-squares program (SigmaPlot) assuming a single class of nonin-

teracting Tus binding sites and a stoichiometry of one molecule of a Tus monomer binding to a single *Ter* site. From these curve fittings, the affinity and standard error of each Tus wt/Tus mutant protein binding to the *Ter* oligonucleotide was determined. The data and standard errors were then replotted as the fraction of *Ter* oligonucleotide shifted as a function of logarithm of the free Tus wt/Tus mutant concentration.

Stability of Tus–Ter Complexes. The relative off-rates for each wt Tus/mutant Tus–*Ter* oligonucleotide interactions were determined from oligonucleotide gel-shift, and band intensities were quantified on a PhosphorImager. The proportion of Ter oligonucleotide released from wt Tus/mutant forms of Tus protein was measured and plotted in the form ln[(Ter oligonucleotide total) − (Ter oligonucleotide free)] versus time (minutes). The slope of the line in this plot approximates $-k_{off}$.

Helicase Assay and Measurement of Off Rate of DNA–Protein Complexes. These were performed as described (5, 20).

Labeling of Kinase-Tagged DnaB and DnaG by Muscle Kinase and [γ^{32}P]-ATP. This procedure was carried out as described (26).

Protein–protein interaction by ELISA and by Glutathione *S*-Transferase (GST) Affinity Columns. The technique has been described (21, 24, 25).

***In Vitro* Replication Assay.** The DNA template contained pUC 18/19-*Ter*80 contained the plasmid *ori* and the left *Ter* site of plasmid R6K located ≈500 nt away from the *ori*. The templates and *in vitro* replication procedures using fraction I of extracts from chloramphenicol-treated *E. coli* have been published (5, 21).

Results

Yeast Forward Two-Hybrid Analysis Revealed Tus–DnaB Interaction *in Vivo*. We wished to investigate possible protein–protein interaction between Tus and DnaB by performing yeast forward two-hybrid analysis (14, 15). To avoid promoter-specific false positives, three separate reporter genes, controlled by three separate promoters, were used (Fig. 3*A*). As shown in Fig. 3 *B* and *C*, the interaction of p53 with simian virus 40 Tag was used as a positive control. As expected, the two proteins interacted readily and strongly, resulting in the yeast cells containing these plasmids to grow on selective plates at 30°C in less than a week. Furthermore, the β-galactosidase activity elicited in these cells was also high. In contrast, cells containing DnaB-pGAD and Tus-pGBT required 10–14 days at 30°C for detectable growth on both the His$^-$ and Ade$^-$ indicator plates. Furthermore, the β-galactosidase activity elicited by Tus–DnaB interaction was low (detectably above the background). Despite this weak interaction, the results were clear and reproducible in multiple experiments. The uniformly positive growth on indicator plates of the Tus–DnaB-containing cells from each colony not only led us to conclude that Tus–DnaB interaction occurs *in vivo* in yeast, but also enabled us to perform reverse two-hybrid analysis as described later. The negative controls using DnaB-pGAD and pGBT vector (without an insert) and the reciprocal were negative for growth on the same indicator plates after 3 weeks of incubation at 30°C (Fig. 3 *B* and *C*). In fact, the reverse two-hybrid experiments served as a most significant piece of additional evidence for the authenticity of Tus–DnaB interaction in the yeast cell milieu.

Tus Did Not Interact with DnaG Primase *in Vivo*. Tus is a basic protein (pI ≈ 8.5), whereas DnaB is acidic (pI ≈ 4.5). Therefore, we had to consider the trivial possibility that the observed interaction could be a nonspecific, acidic protein–basic protein association.

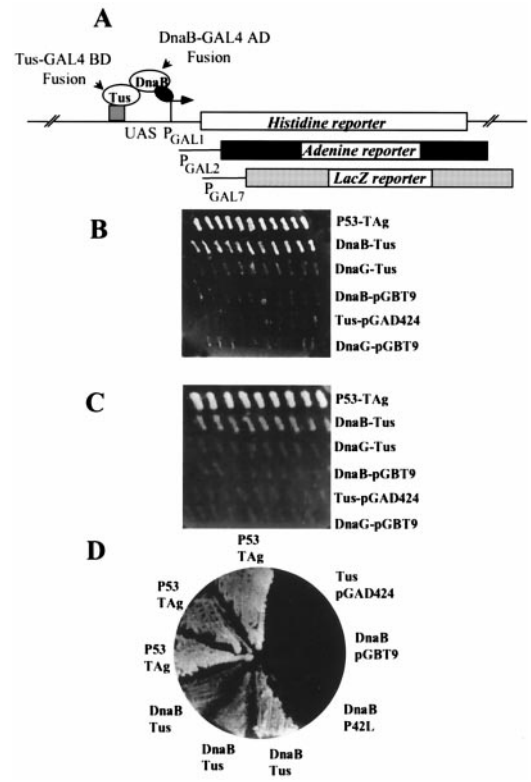

Fig. 3. Forward and reverse two-hybrid analysis of Tus–DnaB interaction. (*A*) Schematic diagram showing the three separate promoters and reporters that were used in this work. (*B*) Photograph of a His$^-$ selection plate showing the relatively luxuriant growth of the cells containing interacting simian virus 40 Tag and p53 proteins. Tus and DnaB interaction elicited consistent but slower growth on the indicator plates. Note that the negative controls containing Tus-DnaG or Tus and DnaB show no growth, even after 2–3 weeks of incubation at 30°C. (*C*) Same as in *B*, excepting that an Ade$^-$ selection plate was used to monitor growth. (*D*) Ade$^-$ plate showing a reverse two-hybrid analysis of a noninteracting Tus mutant P42L and the positive and negative controls.

We eliminated this possibility from further consideration by replacing DnaB with another acidic protein, namely DnaG (pI ≈ 5.0). Two-hybrid analysis indicated that DnaG failed to interact with Tus under the same conditions that promoted DnaB–Tus interaction (Fig. 3 *B* and *C*). The lack of interaction of DnaG with Tus was further confirmed *in vitro* as described later.

Reverse Two-Hybrid Analysis Yielded a Single Noninteracting Missense Mutation in the L1 Loop of Tus. We wished to test not only the specificity of Tus–DnaB interaction but also to obtain noninteracting mutants of Tus by performing reverse two-hybrid analysis. The Tus DNA in the appropriate vector was randomly mutagenized by error-prone PCR and tested for interaction with DnaB. Colonies that failed to grow on both the His$^-$ (plus 2 mM AT) and Ade$^-$ plates were picked and grown in appropriate selective medium to maintain the Tus plasmid and to eliminate the plasmid containing DnaB from the cells. The Tus ORF DNAs present in the plasmids was sequenced. The results showed that 3 of the 5 mutants had a P42L mutation. The other two mutations were outside the ORF. Whereas the p53-Tag and the wt Tus–DnaB-containing cells continued to grow on the indicator plates, P42L Tus failed to elicit reporter gene activity when present with the DnaB-pGBT plasmid in the cells (Fig. 3*D*). It should be noted that P42L mutation is located in the L1 loop of Tus (Figs. 1 and 2).

Wild-Type Tus, but Not the Mutant Forms of Tus, Interacted *in Vitro* with DnaB as Shown by ELISA. We wished to test whether some of the other residues of the L1 loop might be involved in the interaction with DnaB by introducing the mutations E47Q, E49K, and P52L into the DNA encoding Tus, by site-directed mutagenesis (Figs. 1 and 2). The wt and the mutant forms of Tus were expressed, purified to near homogeneity, and tested for various biochemical activities such as protein–protein interaction, DNA binding, and their ability to arrest DnaB helicase and replication forks *in vitro* as described below.

We immobilized wt Tus in the wells of plastic microtiter plates, and after blocking the wells to prevent nonspecific interaction, we incubated the immobilized Tus with various amounts of DnaB in solution. Similarly, immobilized Tus incubated with DnaG in solution was used as a control. The results showed that wt Tus readily interacted with DnaB but not with DnaG, thus confirming the two-hybrid results and providing additional evidence for the specificity of the interaction (Fig. 4 *A* and *B*).

We then immobilized the various mutant forms of Tus in plastic wells and challenged these with various amounts of purified DnaB in solution. The results showed that the P42L protein had largely lost its ability to interact with DnaB, whereas E47Q, E49K, and P52L (Fig. 1) all showed partial but significant loss of interaction with DnaB, in comparison with wt Tus (Fig. 4*A*).

Protein–Protein Interaction by GST Affinity Column Method. We sought to confirm further the interaction described above by an independent method. We fused wt and the various mutant forms of Tus in frame to GST, purified the proteins, and then immobilized equal amounts of the proteins on glutathione-agarose beads. Control beads contained GST only. We labeled kinase-tagged DnaB and DnaG with [γ-^{32}P]ATP and muscle kinase (26) and bound the protein to the affinity matrices containing GST alone or GST-Tus wt/mutant forms. The beads were washed extensively and the bound proteins were eluted and resolved in SDS/PAGE. The data showed that wt Tus bound to the labeled DnaB but the binding was reduced by up to a factor of 8 in the various mutant forms (Fig. 4 *C* and *D*). The labeled DnaG did not bind to the wt Tus-GST matrix above background levels. Thus, the affinity binding data were internally consistent with the ELISA data presented above.

***Ter* DNA-Binding Activities of wt and the Mutant Forms of Tus.** We wished to investigate whether the mutants of the L1 loop were also defective in protein–*Ter* DNA interaction, because the loop contacts DNA sugar phosphate at H50. We proceeded to measure the *Ter*-binding affinities by incubating an equal range of increasing concentrations of wt and the various mutant forms of Tus to a constant amount of labeled *Ter* DNA and resolving the protein–DNA complexes from free DNA by nondenaturing PAGE. The gels were dried and the radioactivity was quantified with a PhosphorImager. The relative K_d (along with the 95% confidence intervals) derived from the binding curves are shown in Table 1. The data show that the E47Q protein appeared to bind to *Ter* DNA somewhat more strongly than did the wt protein. The E49K protein bound to DNA with an affinity that was only $\approx$0.2 $\log_{10}$ less than that of the wt protein. Although P52L appeared to bind to *Ter* almost as well as did E49K, it was clearly a less stable binder as revealed below, by the measurement of its off rate. Although the P42L protein was the weakest binder, it still retained sequence-specific binding to *Ter* DNA (data not shown).

The stability of a DNA–protein complex was measured *in vitro* in the presence of a 200-fold excess of homologous, unlabeled competitor DNA by gel electrophoresis and quantification of the bands of free DNA and DNA–protein complex with a PhosphorImager. The data showed that E49K and E47Q Tus protein–DNA complexes were at least as stable as a wt Tus–*Ter* complex in the presence of competitor DNA (data not shown). In contrast, the P42L protein formed the least stable complex of the group of mutant forms. P52L complex appeared to be more stable than that of P42L but less stable than that of the wt protein.

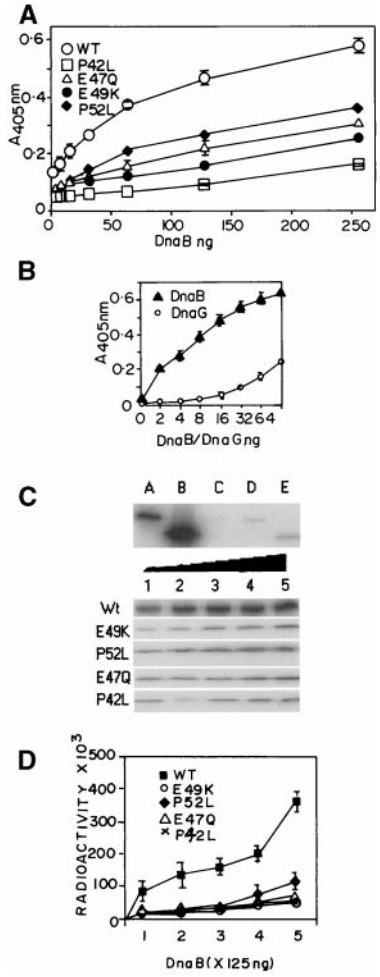

Fig. 4. Confirmation of Tus–DnaB interaction *in vitro* by ELISA and affinity binding. (*A*) ELISA showing the relative binding affinities of immobilized wt and the various mutant forms of Tus to DnaB in solution. (*B*) ELISA (negative control) showing the lack of binding of DnaG in solution to immobilized wt Tus. (*C*) Autoradiogram showing the binding of ^{32}P-labeled DnaB to wt and mutant form of Tus-GST affinity matrices and the lack of binding of labeled DnaG to the wt Tus-GST matrix. GST-affinity matrices containing equal amounts (1 μg) of wt or the various mutant forms of Tus were incubated with an equal, increasing range of concentration of labeled DnaB. The total number of cpm of DnaB added to the matrix in lane E (control) was identical to that added in lane 5 (wt Tus). Note that DnaG (input cpm of DnaG equal to that of DnaB added to lane 5) shows no more than background level of binding to the wt-Tus matrix, consistent with the results shown in *B*. Lanes A and B, input labeled DnaG and DnaB respectively; lanes C and D, DnaG bound to control GST and GST-wt-Tus matrices, respectively; lane E, labeled DnaB bound to control GST matrix; lanes 1–5, increasing and equal range of concentrations of labeled DnaB bound to the wt and the mutant forms of Tus. (*D*) Quantification of three sets of binding data with error bars. Note that DnaB binds up to 8-fold more to the wt Tus matrix in comparison with that to the mutant form Tus-GST matrices.

The Mutant Forms of Tus Failed to Arrest DnaB Helicase *in Vitro*. We prepared partial duplex, helicase substrates consisting of circular M13 single-stranded DNA containing the *Ter* site in both

Table 1. Binding affinities of Tus for *Ter* DNA

Protein	K_d, nM	95% CI
wt	1.5	0.9–2.4
E49K	2.9	2.3–3.7
E47Q	0.4	0.2–0.9
P52L	3.0	2.0–4.6
P42L	5.1	3.5–7.4

CI, confidence interval.

orientations and present in the double-stranded region. The double-stranded region was formed by hybridizing 5′-end-labeled oligonucleotides consisting of the *Ter* sequence to the complementary sequence present on M13 DNA. The partial duplex substrates containing the *Ter* in the blocking and nonblocking orientations were called M13 *Ter* and M13 *Ter*-rev. Helicase assays were performed by using the wt and mutant form of the Tus protein using both the M13 *Ter* and M13 *Ter*-rev, respectively. The wt Tus protein, as expected, arrested DnaB-catalyzed unwinding of M13 *Ter* substrate (Fig. 5) but not of the M13 *Ter*-rev substrate (not shown). The P42L and E49K proteins were almost completely defective in arresting DnaB, whereas P52L was partially defective. Interestingly, although E47Q bound to *Ter* DNA at least as effectively as did the wt Tus and had suffered a reduction in interaction with DnaB, the protein appeared to be nondefective in arresting DnaB helicase *in vitro* (Fig. 5*B*). Because E49K bound to DNA as stably as the wt Tus, this mutant form provides the strongest evidence in support for the involvement of Tus–DnaB interaction in helicase arrest.

The wt and E47Q, but not the E49K, Form of Tus Arrested Replication Forks *in Vitro*. We wished to follow up the reduction in helicase arrest by the mutant forms of Tus by investigating their ability to

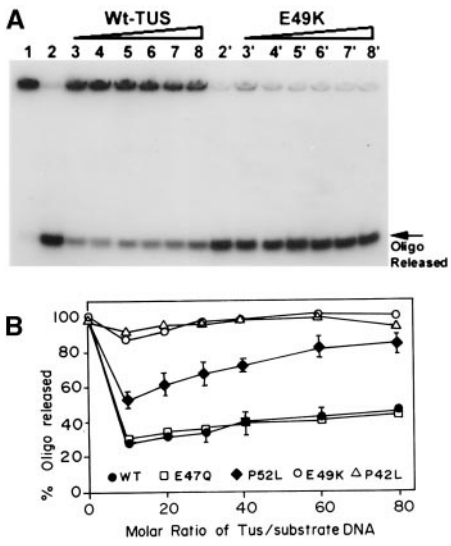

Fig. 5. Helicase-arresting activities of wt and mutant forms of Tus. (*A*) autoradiogram showing the release of melted, labeled oligonucleotide from a partial duplex helicase substrate in the presence of helicase and ATP and with or without an increasing range of concentrations of wt or E49K Tus. The helicase substrate had the Ter sequence in the blocking orientation with respect to the direction of unwinding of DnaB. The wt protein inhibited the unwinding of DNA, whereas the E49K protein was almost completely deficient in arresting DnaB-mediated DNA unwinding. Lane 1, input substrate; lanes 2 and 2′, substrate + DnaB + ATP; lanes 3–8, 10-, 20-, 30-, 40-, 60-, and 80-fold molar excess of Tus over substrate DNA added to the helicase reaction, respectively. Lanes 3′-8′, same as in 3–8 except that the E49K form of Tus was added. (*B*) Quantification of the arrest of helicase-catalyzed unwinding by wt and the various mutant forms of Tus.

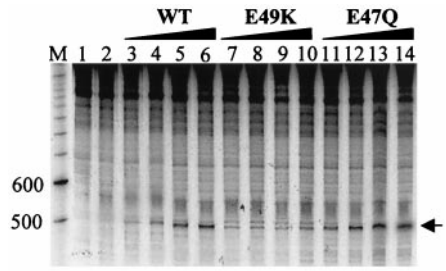

Fig. 6. Autoradiogram showing the relative abilities of wt Tus and the E49K and the E47Q proteins to arrest replication forks *in vitro*. Superhelical pUC18-*Ter*80 template DNA (0.83 pmol) was used in each *in vitro* reaction that included cell extracts from a Tus-deleted *E. coli* (JS117). Lane M, molecular size markers; lanes 1 and 2, *in vitro* replication products without added Tus; lanes 3–7, increasing amounts (1-, 2-, 3-, and 4-fold molar excess of Tus over DNA, respectively) of wt Tus; lanes 7–10, same as in 3–6 except that E49K protein was used; lanes 11–14, same as in 3–7 excepting that E47Q protein was used. The arrow indicates the leading strand that extends from the *ori* and is stalled at the *Ter* site. The numbers on the left refer to number of nucleotides in the marker lane.

arrest replication forks *in vitro*. The wt and the E49K and E47Q mutant forms were selected for the experiments because the two mutant forms did not suffer significant reductions in their affinity for *Ter* DNA. The template pUC18-*Ter*80 was replicated in extracts from *E. coli* JS117 (Tus-deleted) in the presence of [α-^{32}P]dATP as described (5) and the replication products were deproteinized and analyzed in denaturing sequencing gels. The fork arrest at *Ter* was revealed by the appearance of a ≈500-nt band in the autoradiograms. Although wt Tus promoted replication fork arrest at *Ter* (Fig. 6, lanes 3–6), the E49K protein showed a marked reduction in its ability to cause fork arrest (Fig. 6, lanes 7–10), and the the E47Q protein was almost as efficient in promoting fork arrest as the wt protein (Fig. 6, lanes 11–14). Thus, the *in vitro* fork arrest data seemed to be internally consistent with the helicase arrest data (Fig. 5 *A* and *B*).

Discussion

Two alternative hypothesis have been advanced to explain the mechanism of fork arrest by replication terminator proteins: (*i*) formation of a nonspecific roadblock, through the interaction of replication terminator protein with the *Ter* site, that blocks unwinding of DNA duplex by several helicases and RNA polymerases (5–7, 10, 11); and (*ii*) an alternative mechanism that invoked delivery of the Tus protein to the *Ter* site by DNA–protein interaction followed by specific Tus–DnaB protein–protein contact(s). A resolution of the correct mechanism is of importance not only from the perspective of gaining knowledge of replication termination but also for understanding how a helicase unwinds and translocates on DNA. The evidence presented in this paper strongly supports the second model.

Although there never was any real evidence for the roadblock model, the absence of any *in vivo* and *in vitro* evidence for interaction between the arrested and the arresting proteins and the prevalence of mutations in the DNA-binding region of Tus that abolished fork arrest were interpreted as de facto evidence for such a model (9). Although Tus protein is able to arrest DnaB, simian virus 40 Tag (17, 18), and several RNA polymerases (10, 11), it has some helicase specificity, as shown by its inability to arrest helicases involved in rolling circle replication and DNA repair and conjugative transfer (19).

Hitherto, the only *in vivo* evidence, albeit indirect, available for terminator protein–helicase interactions was based mainly on experiments using the replication terminator protein (RTP) of *Bacillus subtilis* (20). There was also some *in vitro* evidence supporting a role of RTP–DnaB interaction in fork arrest (21,

BIOCHEMISTRY

27). Because RTP and Tus have completely different crystal structures (5, 28), it is useful to compare the mechanism in the two systems. Although the polarity of fork arrest in *B. subtilis* appears to be determined at least in part by DNA–protein contacts, in contrast, the asymmetry of Tus protein and DnaB L1-loop contact on the blocking face of Tus determines the polarity in *E. coli* (27). However, both the RTP and the Tus–*Ter* systems involve helicase–contrahelicase interaction (21, 27).

It is interesting to note that the E49K mutant form of Tus, which bound to DNA almost as well as did the wt protein but showed a defect not only in interaction with DnaB helicase but also in arresting the helicase and replication forks *in vitro*, was also obtained in general mutagenesis screens for mutants that were defective in replication termination *in vivo* (8, 12, 13, 29). However, the previous work had provided no real evidence for or against protein–protein interaction between Tus and DnaB, thus failing to illuminate the real mechanism of replication termination.

Although the E49K and E47Q mutations dissociated the DNA-binding activity of Tus from that of its helicase-interacting activity, all of the other mutations examined were defective in not only Tus–DnaB interaction but also in Tus–DNA interaction, presumably because they disrupted the contact between the L1 loop and DNA sugar-phosphate backbone at residue H50. Although the E47Q mutant form did not show any defect *in vitro* in its ability to arrest DnaB helicase in comparison with the wt protein, recent work from another laboratory shows that the mutant form is defective in termination *in vivo* (29).

Do the mutant forms of Tus described here cause only local perturbation of the structure of the L1 loop or a global misfolding of Tus protein? Several lines of reasoning tend to argue against a global folding defect in the mutants, including P42L and P52L, that caused some reductions in Tus–*Ter* interaction. First, the crystal structure data, which show that the L1 loop projects out from the blocking surface of Tus and is flanked by two prolines at 42 and 52, suggest that the L1 loop is probably an independent folding unit. Second, the mutant forms of the protein had almost identical solubility and chromatographic behaviors as the wt protein and showed no evidence of aggregation caused by misfolding. Third, all of the mutant forms retained sequence-specific DNA-binding activity. Therefore, we believe that the mutations in L1 loop probably affected only the local structure of the loop.

Although it is difficult to state at this time whether the L1 is the only motif that contacts the helicase at the blocking face of Tus, and additional points of contacts between Tus and DnaB could not be ruled out at this time, the location of L1 loop at the blocking face suggests a molecular basis of polarity of fork arrest. Helicase approaching from the nonblocking side of Tus could easily displace the protein from the *Ter* DNA and thus pass through unimpeded. In contrast, helicase approaching the blocking face would contact the L1 loop and would be arrested by contact before getting to the DNA-binding region.

It is not clear at this time whether the ATP-hydrolyzing activity of DnaB is abolished and some conformational state of DnaB is changed to cause Tus-mediated arrest. This mechanism will doubtless be the subject of future work. It is also not clear where on DnaB the helicase–contrahelicase contacts occur. Perhaps this problem can be resolved by using the same strategy used in this paper to isolate noninteracting mutants of DnaB.

In a plasmid replicon, absence of a *Ter* site leads to rolling circle replication and consequent plasmid instability *in vivo* (22). *In vitro*, the Tus–*Ter* complex seems to prevent over-replication of *oriC* (23). Beyond these observations, little is known about the physiological role of the Tus–*Ter* system *in vivo*, despite their ubiquitous presence in prokaryotic chromosomes. This aspect of replication termination should also be a subject of future work.

We thank Dr. B. K. Mohanty for performing the first ELISA and some of the *in vitro* replication experiments. This work was supported by a grant from the National Institute of General Medical Sciences and a Merit Award from the National Institute of Allergy and Infectious Diseases (to D.B.).

1. Bastia, D. & Mohanty, B. K. (1996) in *DNA Replication in Eukaryotic Cells*, ed. DePamphilis, M. (Cold Spring Harbor Lab. Press, Plainview, NY), pp. 177–215.
2. Bussiere, D. E. & Bastia, D. (1999) *Mol. Microbiol.* **31,** 1611–1618.
3. Horiuchi, T. & Hidaka, M. (1988) *Cell* **54,** 515–523.
4. Hill, T. M., Pelletier, A. J., Tecklenberg, M. L. & Kuempel, P. L. (1988) *Cell* **55,** 459–466.
5. Khatri, G. S., MacAllister, T., Sista, P. & Bastia, D. (1989) *Cell* **59,** 667–674.
6. Lee, E. H., Kornberg, A., Hidaka, M., Kobayashi, T. & Horiuchi, T. (1989) *Proc. Natl. Acad. Sci. USA* **86,** 9104–9108.
7. Hiasa, H. & Marians, K. (1992) *J. Biol. Chem.* **267,** 11379–11385.
8. Kamada, K., Horiuchi, T., Ohsumi, K., Shimamoto, M. & Morikawa, K. (1996) *Nature (London)* **383,** 598–603.
9. Yamamoto, K. R. & Alberts, B. M. (1976) *Annu. Rev. Biochem.* **45,** 721–746.
10. Mohanty, B. K., Sahoo, T. & Bastia, D. (1996) *EMBO J.* **15,** 2532–2539.
11. Mohanty, B. K., Sahoo, T. & Bastia, D. (1998) *J. Biol. Chem.* **273,** 3051–3059.
12. Skokotas, A., Wrobelski, M. & Hill, T. (1994) *J. Biol. Chem.* **269,** 20446–20455.
13. Skokotas, A., Hiasa, H., Marians, K. J., O'Donnell, L. & Hill, T. M. (1995) *J. Biol. Chem.* **270,** 30941–30948.
14. Fields, S. & Song, O. S. (1989) *Nature (London)* **340,** 245–246.
15. James, P., Halladay, J. & Craige, C. A. (1996) *Genetics* **144,** 1425–1436.
16. Wake, R. G. & King, G. (1997) *Structure* **5,** 1–5.
17. Bedrosian, C. & Bastia, D. (1991) *Proc. Natl. Acad. Sci. USA* **88,** 2618–2622.
18. Amin, A. A. & Hurwitz, J. (1992) *J. Biol. Chem.* **267,** 18612–18622.
19. Sahoo, T., Mohanty, B. K. & Bastia, D. (1995) *J. Biol. Chem.* **270,** 29138–29144.
20. Gautam, A. & Bastia, D. (2001) *J. Biol. Chem.* **276,** 8771–8777.
21. Manna, A. C., Pai, K. S., Bussiere, D. E. & Bastia, D. (1996) *Cell* **87,** 881–891.
22. Krabbe, M., Zabielski, J., Bernander, R. & Nordstrom, K. (1997) *Mol. Microbiol.* **24,** 723–735.
23. Hiasa, H. & Marians, K. (1994) *J. Biol. Chem.* **267,** 16371–16375.
24. Ratnakar, P. V. A. L., Mohanty, B. K., Lobert, M. & Bastia, D. (1996) *Proc. Natl. Acad. Sci. USA* **93,** 5522–5526.
25. Lu, Y.-B., Ratnakar, P. V. A. L., Mohanty, B. K. & Bastia, D. (1996) *Proc. Natl. Acad. Sci. USA* **93,** 12902–12907.
26. Yuzhakov, A., Turner, J. & O'Donnell, M. (1996) *Cell* **86,** 877–886.
27. Gautam, A., Mulugu, S., Alexander, K. & Bastia, D. (2001) *J. Biol. Chem.* **276,** 23471–23479.
28. Bussiere, D. E., Bastia, D. & White, S. (1995) *Cell* **80,** 651–660.
29. Henderson, T. F., Nilles, A. F., Valjavoc-Gratian, M. & Hill, T. M. (2001) *Mol. Gen. Genet.*, in press.